



SHORT-TERM LOAD FORECASTING OF REGIONAL INTEGRATED ENERGY SYSTEM

*J. Wang**

Abstract: Based on the theoretical analysis of Elman network, the short-term load forecasting model of regional integrated energy system is established. The structure and parameters of the model are determined through repeated off-line training and experiments. The forecasting accuracy is significantly higher than that of traditional BP network, and the prediction error is less than 3%, which can meet the needs of coordination and scheduling of regional integrated energy system.

Key words: *short-term load forecasting, ENN, BP network, regional integrated energy system*

Received: April 12, 2020

DOI: 10.14311/NNW.2021.31.023

Revised and accepted: December 31, 2021

1. Introduction

The regional integrated energy system (RIES) can concentrate a variety of complementary distributed energy in the same network. It can improve the energy utilization, economy and stability of the whole regional energy system by using clean energy such as solar energy, geothermal energy, air energy, natural gas and wind energy. It can be applied to various parks, public buildings, industrial enterprises and other scenarios [1]. However, due to the uncertainty of clean energy output and load demand in RIES, it brings huge risks and challenges to ensure the stable and energy saving operation of RIES, robust optimal scheduling must be adopted [2]. Short-term load forecasting (STLF) is the premise for the robust optimal scheduling of RIES [3]. The production and consumption of energy is undergoing profound changes with the progress of technology and the improvement of people's living standard and the coupling between energy sources is becoming stronger and stronger, which puts forward higher requirements for the accuracy and timeliness of STLF [4].

Many classical methods were used to study STLF, such as support vector machine [5], neural network [6, 7] and statistical methods [8–10]. Because of its strong learning and mapping energy, neural network can simulate complex nonlinear relationships with arbitrary accuracy, and it has become an important calculation

*JianYu Wang; School of Equipment Engineering, Jiangsu Urban and Rural Construction College, Jiangsu Changzhou 213147, China, E-mail: 28210646@qq.com

tool for STLF [11]. The load of the system is not only affected by the external weather and user usage, but also closely related to the load at the previous time. This dynamic nature of load determines that static neural networks, such as radial basis function (RBF) neural network, back propagation (BP) neural network and wavelet neural network (WNN), cannot achieve the best effect [12].

Elman neural network (ENN) is a neural network formed by adding a context layer on the basis of BP neural network. It is a dynamic model that can remember the historical state. On each iteration, the context layer of ENN can feed back the error to the input layer, and correct the input data of the input layer according to the feedback error to reduce the error. Compared with BP neural network, ENN has higher prediction accuracy [13]. In this paper, ENN is used to predict the electric and heat or cooling load of regional integrated energy system, and the prediction results are compared with BP neural network.

2. Elman neural network (ENN)

2.1 The structure of ENN

As shown in Fig. 1, ENN forms a new generation of neural network by adding a context layer on the basis of the traditional neural network composed of input layer, hidden layer and output layer. The neurons in the context layer are the same as those in the hidden layer. The hidden layer outputs the data to the output layer after weighted processing, and stores the data in the context layer. The data stored in the context layer is input back to the hidden layer together with the data of the next group of input layers, so as to reuse the data of the hidden layer and form a recursive network [14].

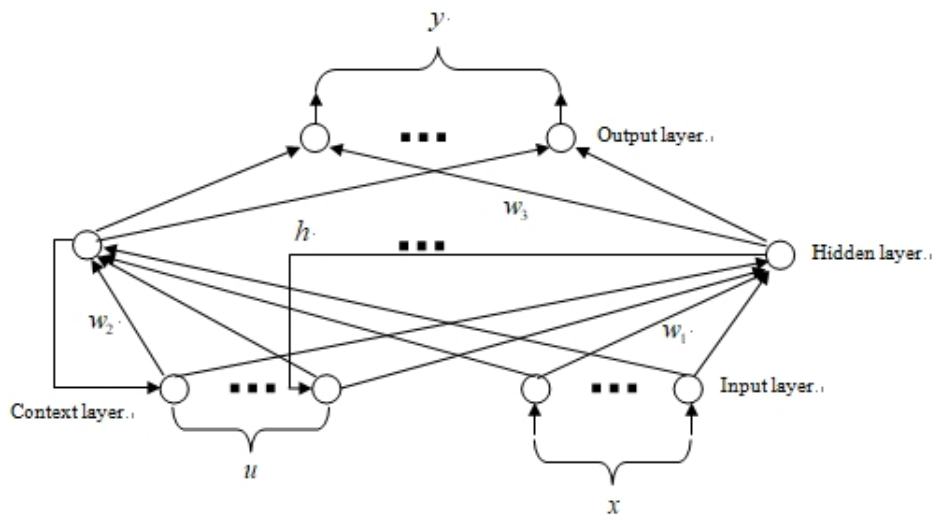


Fig. 1 The structure of Elman neural network.

In Fig. 1, the ENN has an n -dimensional input layer, and the input vector at time t is $x(t) = [x_1(t), x_2(t), \dots, x_n(t)]$. The number of neurons between the hidden layer and the context layer is m , and they correspond to each other one by one. The vector of the context layer is $u(t) = [u_1(t), u_2(t), \dots, u_m(t)]$, and the vector of the hidden layer is $h(t) = [h_1(t), h_2(t), \dots, h_m(t)]$. In order to increase the nonlinearity of the neural network model, sigmoid function is selected as the activation function, and $h(t)$ can be calculated according to the following formula:

$$h_i(t) = f(v_i^h(t)) = \frac{1}{1 + \exp(-v_i^h(t))}, (i = 1, 2, \dots, m), \quad (1)$$

$$v_i^h(t) = \sum_{j=1}^n w_{1ij}(t)x_j(t) + \sum_{j=1}^m w_{2ij}(t)u_j(t), (i = 1, 2, \dots, m), \quad (2)$$

$$u_j(t) = x_j(t-1), (j = 1, 2, \dots, m). \quad (3)$$

Here, $w_1(t) \in R^{n \times m}$ is the weight matrix from the input layer to the hidden layer and $w_2(t) \in R^{m \times m}$ is the weight matrix of context layer to hidden layer.

Fig. 1 contains a k -dimensional output layer, and the output vector is expressed as $y(t) = [y_1(t), y_2(t), \dots, y_k(t)]$, here t indicates t th output sequence. $y(t)$ can be computed by equations below:

$$y_i(t) = f(v_i^o(t)) = \frac{1}{1 + \exp(-v_i^o(t))}, (i = 1, 2, \dots, k), \quad (4)$$

$$v_i^o(t) = \sum_{j=1}^m w_{3ij}(t)h_j(t), (i = 1, 2, \dots, k). \quad (5)$$

Here, $w_3(t) \in R^{m \times k}$ is the weight matrix of hidden layer to output layer.

2.2 Learning algorithm of ENN

Assuming that the actual output of the system is $d(t)$, the error between the predicted value and the actual value of ENN is:

$$E(t) = \frac{1}{2}(d(t) - y(t))^T(d(t) - y(t)). \quad (6)$$

In order to minimize the error, the gradient descent method is adopted. When the partial derivative of $E(t)$ to the weight is equal to 0, the learning algorithm of ENN can be obtained [15]:

$$\Delta w_{3ij}(t) = \eta_3 h_i(t)(d_j(t) - y_j(t))f'(v_i^o(t)), (i = 1, 2, \dots, m)(j = 1, 2, \dots, k), \quad (7)$$

$$\Delta w_{2ij}(t) = \eta_2 \sum_{l=1}^k (w_{3il}(d_j(t) - y_j(t))f'(v_i^o(t)))f'(v_i^h(t))h_j(t-1) \quad (8)$$

$$(i = 1, 2, \dots, m; j = 1, 2, \dots, m),$$

$$\Delta w_{1ij}(t) = \eta_1 x_i(t) \sum_{l=1}^k (w_{3il}(d_j(t) - y_j(t))f'(v_i^o(t)))f'(v_i^h(t)) \quad (9)$$

$$(i = 1, 2, \dots, n; j = 1, 2, \dots, m),$$

here, η_1 , η_2 and η_3 are the learning rates of the w_1 , w_2 and w_3 respectively.

2.3 Model evaluation

In order to determine the parameters of the model according to the prediction accuracy of the model, the model average absolute percentage error (*MAPE*) of the predicted value and the actual value is usually used to evaluate the prediction effect of the model [16]:

$$MAPE_k = \frac{1}{N} \sum_{i=1}^N \left| \frac{y_{ki} - \hat{y}_{ki}}{y_{ki}} \right|. \quad (10)$$

Here y_{ki} and \hat{y}_{ki} , ($k = 1, 2$) represent the predicted and actual values of the electric and heat or cooling load respectively, N is the number of samples. If the weights of electric end thermal loads (or cooling load) are set to 0.6 and 0.4 respectively, the average prediction accuracy (*MA*) is:

$$MA = 0.6 \times (1 - MAPE_1) + 0.4 \times (1 - MAPE_2). \quad (11)$$

3. Short-term load forecasting

3.1 Prediction process

According to the historical data, weather data, course information and school calendar data provided by the campus data platform of Jiangsu urban and rural construction vocational college, the short-term load is learned offline and predicted online by using ENN. The prediction process is shown in Fig. 2.

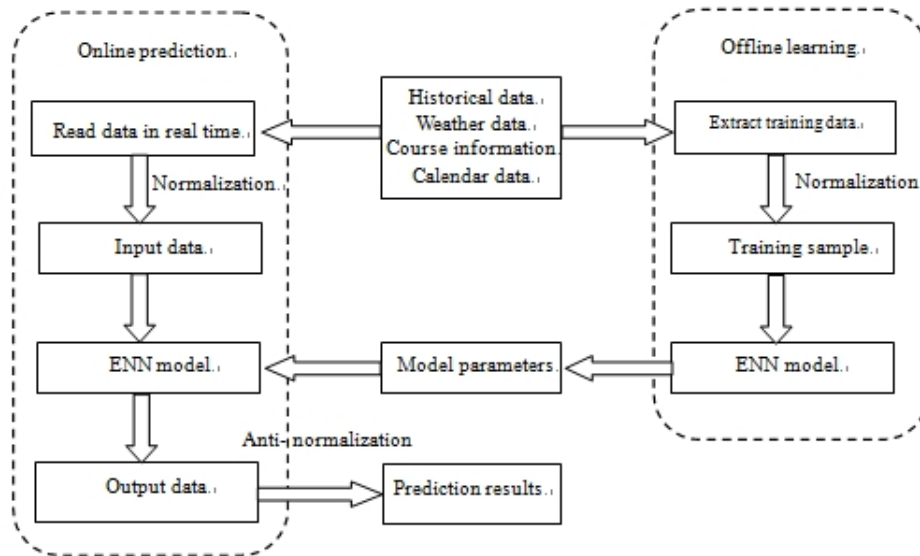


Fig. 2 Short-term load forecasting process of regional integrated energy system.

Through off-line training, the system determines the parameters of the ENN model, and then forecasts the current electric, heat and cooling load through the

real-time reading data. In order to effectively coordinate and mobilize the energy system according to the demand side demand, the prediction is made at the interval of one hour.

3.2 Sample data and preprocessing

Through the analysis of the data association of the college data platform in 2018, the main factors affecting the load are taken as the input data, including:

- Historical data: the electric and heat or cooling load at the previous moment (x_1, x_2); the electric and heat or cooling load at the same time of the previous day (x_3, x_4), and the electric and heat or cooling load at the same time of the previous week (x_5, x_6).
- Weather data: current outdoor air temperature (x_7) and relative humidity (x_8).
- Course information: number of practical courses (x_9) and theoretical courses (x_{10}) of the day.
- School calendar data: x_{11} takes 1,2 and 3 as teaching day, weekend and holiday separately.
- Output data: current electric and thermal load (y_1, y_2).

Before running ENN for off-line learning and on-line prediction, all data must be linearly normalized to the range $[-1, 1]$. The normalization method of input and output data is as follows [17]:

$$x_i^n = \frac{x_i - \bar{x}_i}{\sigma_i}, \quad (12)$$

$$y_j^n = \frac{y_j - \bar{y}_j}{\sigma_j}, \quad (13)$$

where \bar{x}_i and $\sigma_i (i = 1, 2, \dots, 11)$ are the mean and standard deviation of input variable samples, \bar{y}_j and $\sigma_j (j = 1, 2)$ are the mean and standard deviation of output variable samples.

3.3 Model selection and training

In order to predict the electric and cooling load of the system, 960 samples (sampling time 1 hour) from September 1 to October 10, 2018 are selected for offline learning, of which 720 samples from September 1 to 30, 2018 are the training set and 240 samples from October 1 to 10, 2018 are the verification set. In order to predict the electrical and heat load of the system, 960 samples (sampling time 1 hour) from December 2, 2018 to January 10, 2019 are selected for offline learning, of which 720 samples from December 1 to 31, 2018 are the training set and 240 samples from January 1 to 10, 2019 are the verification set. All data come from the data platform of Jiangsu urban and rural construction vocational college. The learning rate is set to 0.1 and the number of iterations is set to 2,000. In Elman neural network, the number of hidden neurons directly determines the prediction effect [18]. The results of the two sample sets with several different numbers of

neurons in the hidden layer are shown in Tab. I. The training results of both samples show that the Elman network with 22 hidden units (and 22 context units) is the best in average prediction accuracy (*MA*).

The number of neurons	11	22	33	44
<i>MA</i> (cooling load)	0.9318	0.9768	0.9234	0.9012
<i>MA</i> (heat load)	0.9215	0.9644	0.9184	0.9088

Tab. I The relationship between the number of neurons in the hidden layer and the prediction accuracy.

The hidden units (and context units) are set to 22. The change of training and verification set accuracy during ENN iteration during electric and cooling load forecasting of the system is shown in Fig. 3. The change of training and verification set accuracy during ENN iteration during electric and heat load forecasting of the system is shown in Fig. 4. The accuracy obtained meets the engineering requirements.

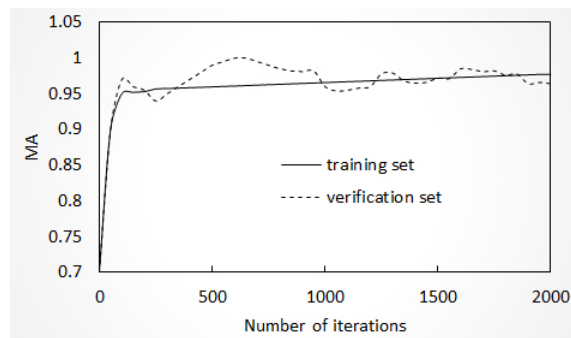


Fig. 3 The change of training and verification set accuracy during ENN iteration during electric and cooling load forecasting of the system.

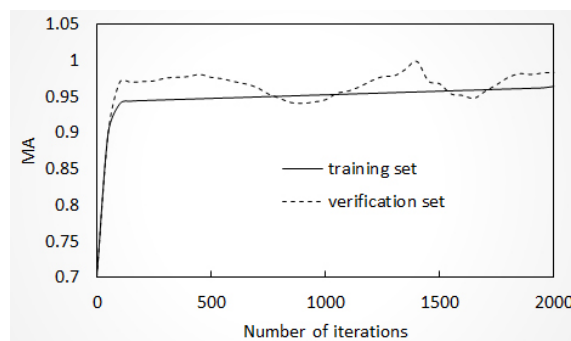


Fig. 4 The change of training and verification set accuracy during ENN iteration during electric and heat load forecasting of the system.

When 22 neurons are selected in the hidden layer and the number of iterations is 2,000, the verification set is shown in Fig. 5 – Fig. 8. Tab. II shows the *MAPE* between the predicted and measured values using ENN and BP neural networks

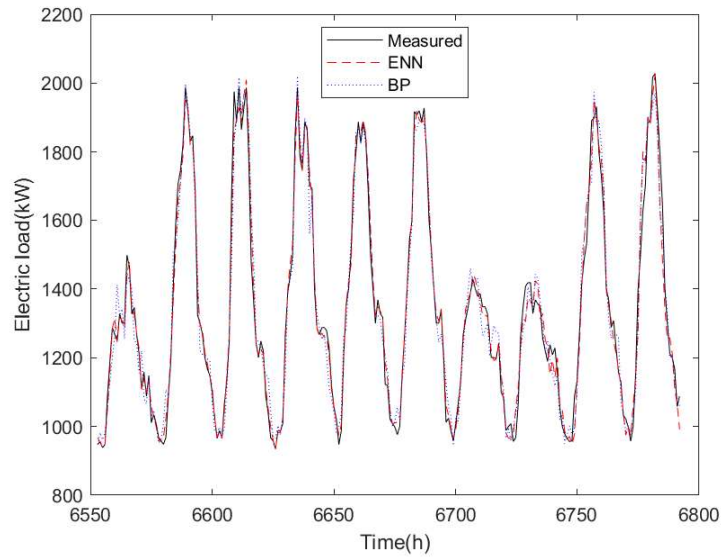


Fig. 5 Verification of electric load forecasting from October 1 to 10, 2018.

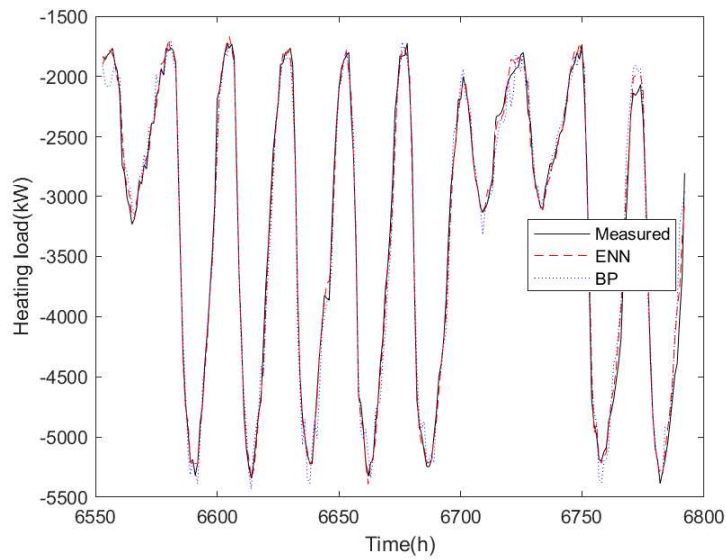


Fig. 6 Verification of cooling load forecasting from October 1 to 10, 2018.

during validation. Compared with BP neural network, ENN not only reduces the *MAPE* of predicted and measured value by more than 1%, but also has stronger computing power and network stability.

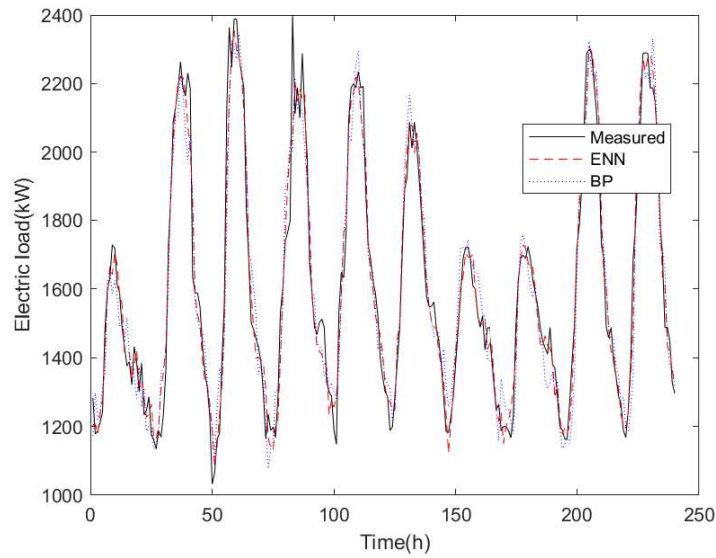


Fig. 7 Verification of electric load forecasting from January 1 to 10, 2019.

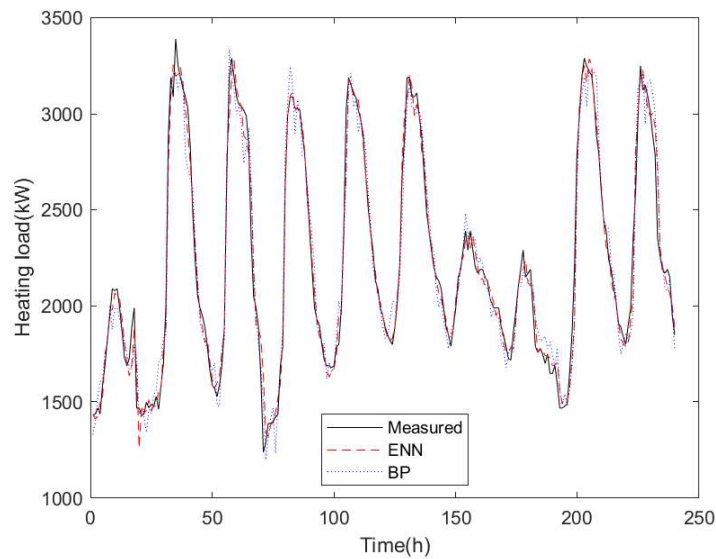


Fig. 8 Verification of heat load forecasting from January 1 to 10, 2019.

Time interval	October 1–10, 2018		January 1–10, 2019	
Load type	Electric load	Cooling load	Electric load	Heat load
ENN <i>MAPE</i> (%)	2.3208	2.0919	2.4450	2.1250
BP <i>MAPE</i> (%)	4.1877	3.4553	4.2419	4.0865

Tab. II Average absolute percentage error between predicted value and measured value.

4. Prediction results and analysis

In order to verify the prediction performance of ENN model in the process of rapid climate change, the electric and heat load from March 1 to 14, 2019 are predicted after rolling training of the model. The prediction results are shown in Fig. 9–Fig. 10, in which the actual load value and BP neural network prediction value are listed for comparison. Due to the great climate change, the *MAPE* of electric load prediction is 2.701%, and that of heat load prediction is 2.355%. The predicted *MAPE* is higher than the verified *MAPE*, but about 2% lower than that predicted by BP neural network. Due to the influence of random factors, the *MAPE* of electric load prediction and measurement is larger than that of heat loads, but not more than 3%, which meets the requirements of short-term load prediction and can be used for the coordinated dispatching of regional energy Internet energy system [19].

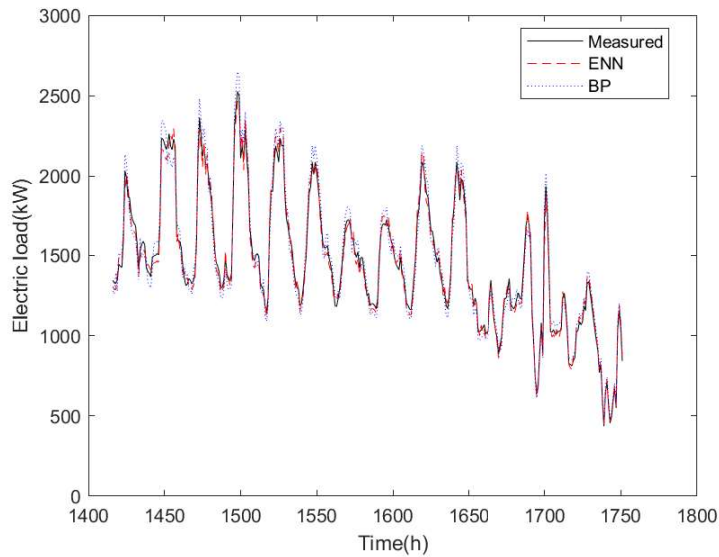


Fig. 9 Electric load forecast from March 1 to 14, 2019.

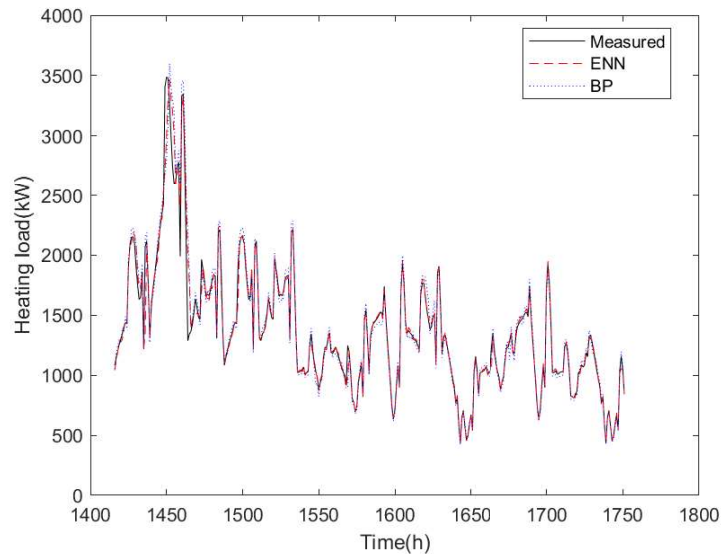


Fig. 10 Heating load forecast from March 1 to 14, 2019.

5. Conclusion

In this paper, a short-term load forecasting method of regional Internet energy system based on ENN is proposed. By setting the parameters and structure of the model, and using the data from the data platform of Jiangsu urban and rural construction vocational college to train the model, the electric and heat loads of the campus are predicted. The following conclusions can be drawn from the research:

- The short-term load of regional integrated energy system is not only related to meteorological data, data characteristics and regional activities, but also closely related to time series. This dynamic characteristic of load can not be well predicted by static neural network. Selecting ENN with dynamic regression characteristics not only improves the computing electric of the network and the stability of system operation, but also reduces the *MAPE* of prediction by 2% compared with the traditional BP network.
- The prediction accuracy of ENN is closely related to the network structure parameters such as the number of neurons in the hidden layer and the receiving layer. When there are few neurons in the hidden layer, the calculation time is short, but the prediction accuracy is low; When there are many hidden layer neurons, not only the calculation time is very long, but also the prediction accuracy is low. Experiments show that the prediction accuracy is the highest when the number of hidden layer neurons is about twice the number of input variables.
- When using ENN model to predict the short-term load of RIES, due to many uncertain factors of electric load, the *MAPE* between the predicted value and

the actual value is large, but not more than 3%, which can meet the needs of coordinated dispatching of regional integrated energy system.

Acknowledgement

This work was supported by the Construction system science and technology project of Jiangsu province of China (No. 2018ZD224).

References

- [1] XU B., ZHANG Y. Development path of regional integrated energy system. *Earth and Environmental Science*. 2019, 371(3), pp. 042034, doi: [10.1088/1755-1315/371/4/042034](https://doi.org/10.1088/1755-1315/371/4/042034).
- [2] LIU L., WANG D., HOU K., JIA H., LI S. Region model and application of regional integrated energy system security analysis. *Applied Energy*. 2020, 260, pp. 114268, doi: [10.1016/j.apenergy.2019.114268](https://doi.org/10.1016/j.apenergy.2019.114268).
- [3] SHIJU W., KE X., JING X., FUJIAN C., XUEFEI Z., LIANG Z. Comprehensive theoretical and evaluation system of integrated energy system. *Earth and Environmental Science*. 2018, 168(1), pp. 012035.
- [4] JIA J., ZENG M. Research on Constructing Integrated Energy System. *Earth and Environmental Science*. 2019, 300(4), pp. 042042, doi: [10.1088/1755-1315/300/4/042042](https://doi.org/10.1088/1755-1315/300/4/042042).
- [5] NIU D., WANG Y., WU D.D. Power load forecasting using support vector machine and ant colony optimization. *Expert Systems with Applications*. 2010, 37(3), pp. 2531–2539, doi: [10.1016/j.eswa.2009.08.019](https://doi.org/10.1016/j.eswa.2009.08.019).
- [6] KHWAJA A.S., NAEEM M., ANPALAGAN A., VENETSANOPOULOS A., VENKATESH B. Improved short-term load forecasting using bagged neural networks. *Electric Power Systems Research*. 2015, 125, pp. 109–115, doi: [10.1016/j.epsr.2015.03.027](https://doi.org/10.1016/j.epsr.2015.03.027).
- [7] HIPPERT H., PEDREIRA C., SOUZA R. Neural networks for short-term load forecasting: a review and evaluation. *IEEE Transactions on Power Systems*. 2001, 16(1), pp. 44–55, doi: [10.1109/59.910780](https://doi.org/10.1109/59.910780).
- [8] CHARYTONIUK W., CHEN M.S., OLINDA P.V. Neural networks for short-term load forecasting: a review and evaluation. *IEEE Transactions on Power Systems*. 1998, 13(3), pp. 725–730, doi: [10.1109/59.708572](https://doi.org/10.1109/59.708572).
- [9] MASTOROCOSTAS P.A., THEOCHARIS J.B., KIARTZIS S.J., BAKIRTZIS A.G. A hybrid fuzzy modeling method for short-term load forecasting. *Mathematics and Computers in Simulation*. 2000, 51(3), pp. 7221–232, doi: [10.1016/S0378-4754\(99\)00119-6](https://doi.org/10.1016/S0378-4754(99)00119-6).
- [10] SONG K.B., BAEK Y.S., HONG D.H., JANG G. Short-term load forecasting for the holidays using fuzzy linear regression method. *IEEE Transactions on Power Systems*. 2005, 20(1), pp. 96–101, doi: [10.1109/TPWRS.2004.835632](https://doi.org/10.1109/TPWRS.2004.835632).
- [11] Zhang Z, Gong W. Short-Term Load Forecasting Model Based on Quantum Elman Neural Networks. *Mathematical Problems in Engineering*. 2016, doi: [10.1155/2016/7910971](https://doi.org/10.1155/2016/7910971).
- [12] LI P., LI Y., XIONG Q., CHAI Y., ZHANG Y. Application of a hybrid quantized Elman neural network in short-term load forecasting. *International Journal of Electrical Power and Energy Systems*. 2014, 55, pp. 749–759, doi: [10.1016/j.neucom.2019.02.063](https://doi.org/10.1016/j.neucom.2019.02.063).
- [13] ALKHASAWNEH M.S. Hybrid Cascade Forward Neural Network with Elman Neural Network for Disease Prediction. *Arabian Journal for Science and Engineering*. 2019, 44(11), pp. 9209–9220, doi: [10.1007/s13369-019-03829-3](https://doi.org/10.1007/s13369-019-03829-3).
- [14] XIE K., YI H., HU G., LI L., FAN Z. Short-term power load forecasting based on Elman neural network with particle swarm optimization. *Neurocomputing*. 2019, doi: [10.1016/j.neucom.2019.02.063](https://doi.org/10.1016/j.neucom.2019.02.063).
- [15] REN G., CAO Y., WEN S., HUANG T., ZENG Z. A modified Elman neural network with a new learning rate scheme. *Neurocomputing*. 2018, 286, pp. 11–18, doi: [10.1016/j.neucom.2018.01.046](https://doi.org/10.1016/j.neucom.2018.01.046).

- [16] MARVUGLIA M., MESSINEO A. Using recurrent artificial neural networks to forecast household electricity consumption. *Energy Procedia*. 2012, 14, pp. 45–55, doi: [10.1016/j.egypro.2011.12.895](https://doi.org/10.1016/j.egypro.2011.12.895).
- [17] YA-LAN Y., YAO-LIANG X., SHAO-SHUN Z., JIANG-YUAN X. MRA-SVM Model of Forecasting for Wind Speed in Short-term. *Proceedings of the CSU-EPSCA*. 2014, 26(5), pp. 44–49.
- [18] BECCALI M., CELLURA M., LO BRANO V., MARVUGLIA A. Short-term prediction of household electricity consumption: Assessing weather sensitivity in a Mediterranean area. *Renewable and Sustainable Energy Reviews*. 2008, 12(8), pp. 2040–2065, doi: [10.1016/j.rser.2007.04.010](https://doi.org/10.1016/j.rser.2007.04.010).
- [19] MUZAFFAR S., AFSHARI A. Short-Term Load Forecasts Using LSTM Networks. *Energy Procedia*. 2019, 158, pp. 2922–2927, doi: [10.1016/j.egypro.2019.01.952](https://doi.org/10.1016/j.egypro.2019.01.952).